

**High productive and continuous nanoparticle fabrication
by laser ablation of a wire-target in a liquid jet**

**Sebastian Kohsakowski^{1,2}, Antonio Santagata³, Marcella Dell'Aglio⁴,
Alessandro de Giacomo^{4,5}, Bilal Gökce^{1*}, Stephan Barcikowski^{1,2} and Philipp
Wagener^{1,2}**

¹ *University of Duisburg-Essen, Technical Chemistry I and Center of Nanointegration Duisburg-Essen (CENIDE), Universitätsstrasse 7, Essen, D-45141 Germany*

² *NanoEnergieTechnikZentrum – NETZ, Carl-Benz-Straße 199, Duisburg, D-47057, Germany.*

³ *CNR-ISM, UOS Tito Scalo - C.da S. Loja - Zona Industriale, Tito Scalo (PZ), I-85050, Italy.*

⁴ *CNR-NANOTEC, Via Amendola 122/D, Bari, I-70126, Italy*

⁵ *Department of Chemistry, University of Bari “Aldo Moro”, Via Orabona 4, Bari, Italy*

*contact author: bilal.goekce@uni-due.de

Tel.: +49 2011 83146

Fax: +49 2011 83049

E-Mail contacts:

Sebastian.Kohsakowski@uni-due.de

Antonio.santagata@cnr.it

Marcella.dellaglio@ba.cnr.it

Alessandro.degiacomo@nanotec.cnr.it

Stephan.Barcikowski@uni-due.de

Philipp.Wagener@uni-due.de

Keywords

Silver NPs, Wire ablation, NPs productivity, shielding effect, cavitation bubble dynamics

Abstract

To scale-up pulsed laser ablation in liquids for nanoparticle synthesis, we combined two promising approaches, a wire shaped target and a small liquid layer, in one setup. Using thin liquid layers a significant increase in nanoparticle productivity (up to 5 times) has been obtained. The increase of nanoparticle productivity can be attributed to the dynamics, shape of the cavitation bubble and the spring-board like behavior of the wires in the small liquid filament. In addition to the cavitation bubble further shielding effects have been related to both, the laser ablated material and the presence of generated small vapor bubbles. The obtained results show that this setup can provide a good strategy to realize a continuous ablation process approaching without the need of target replacement towards industrial scale applications.

Introduction

The interest in nanoparticles (NPs) and nanocomposites has grown exponentially over the recent years due to their one-of-a-kind properties and their unique applications. Currently, most of the NPs are generated with conventional methods such as gas phase synthesis^{1, 2} wet chemical synthesis^{3, 4} but also with milling⁵. However, limitations and disadvantages arise when nanoparticles are synthesized with any of these techniques. For the gas phase synthesis of NPs cost-intensive precursor as feedstock are necessary and the NPs aggregate during capturement. Purity of these nanoparticles is one of these limitations, because grinding media, chemical precursors, surfactants or reducing agents^{3, 4} are required to generate the NPs. These additives or the abrasion of the grinding media may interact with the NP surface⁶ causing impurity layer formation. For many applications like catalysis^{7, 8} and biomedicine⁹ pure ligand-free NPs are extremely demanded because of the absence of a catalytic-activity-limiting or toxic ligands that don't need to be cleaned with methods such as thermal treatment¹⁰ or centrifugation¹¹ that may alter the nanoparticle properties.

A technique to synthesize pure ligand-free colloidal NPs is pulsed laser ablation in liquids (PLAL). In comparison with other synthesis routes the variability of materials and liquids is extremely diverse. It is possible to obtain NPs from metals¹², alloys¹³⁻¹⁶ and ceramics^{6, 17} from many target shapes (foil¹⁸, wire^{19, 20}, pressed powder¹⁵). Despite these many advantages, PLAL still shows one major drawback; its low productivity compared to industrially established methods. The NP productivity (i.e. yield of NPs generated per unit of time, commonly measured by mg/h) that can be obtained by PLAL is low due to several reasons one being that most of the PLAL setups are discontinuous. Therefore, new strategies and methods have to be developed to realize high NP productivities in a continuous process. These strategies can be divided into cost-

intensive and non-cost-intensive methods. Cost-intensive parameters that lead to an increase in NP productivity are laser power and scanning speed.²¹⁻²³ Sajti et al.²⁴ reported an increase in ablation rate (but did not quantify NP productivity directly) for higher pulse energies and fluences using a ns-laser system while Streubel et al.^{25, 26} recently showed productivities of 4g/h for a 500W ps-laser system that additionally utilized a polygon scanner. In both cases the increase is connected to higher laser systems costs. The importance of non-cost-intensive methods to increase the productivity of PLAL has been demonstrated by several research groups pursuing different strategies.^{20, 27, 28} The most important non-cost-intensive methods can be categorized in methods that utilize or alter: (i) beam guiding^{17, 28}, (ii) liquid properties^{27, 29}, (iii) target-shape^{20, 30} and (iv) laser properties (wavelength, intensity)³¹.

However, all these methods are somehow related to the fundamentals of PLAL. During the ablation process a cavitation bubble is formed on the target-surface induced by the laser pulse. When laser pulses with high repetition rates are used the formed cavitation bubbles can lead to a shielding of the successive laser pulses. This results in a loss of the effective laser energy reaching the target and hence reduced the productivity. Sasaki et al.³² and De Giacomo et al.³³ showed that the lifetime (that depends on the pulse energy and liquid properties) of the cavitation bubble, in case of a confining liquid, may extend up to several hundred microseconds with a spatial elongation reaching some millimetres (at high pulse energies). During the cavitation bubble lifetime, the bubble can interact with subsequent laser pulses which cause a shielding of laser intensity. This phenomenon is especially observed for high repetition rates of the laser, where the cavitation bubble lifetime is in the same order of magnitude as the temporal laser interpulse delay. Several studies reported the influence of the interpulse delay time, or lateral distance between two pulses, on the NP productivity. In fact, a maximum in productivity was observed at distances of 125 μm (500 mm/s scan speed)^{17, 24} and 175 μm bypassing the generated

cavitation bubbles by using a fast beam guidance²⁸. Very high repetition rates in MHz regime require lateral scan speeds around 500 m/s to achieve maximum productivities.^{25, 26} Moreover, the NP productivity is increased by changing the properties of the liquid. This can be optimized by a liquid flow³⁴ and by the variation of the liquid film thickness^{27, 29}. Barcikowski et al.³⁴ observed an increase of the NP productivity by 380 % in case of a liquid flow setup in comparison with a stationary setup. The enhanced productivity was ascribed to a faster removal of the generated NPs and the small vapor bubbles self-generated during the process which can interact with the laser beam.³⁴ Hence, in order to enhance the NP productivity PLAL is performed more frequently in liquid flow.

Another parameter that is related to fluidics is the liquid film thickness, which increases the PLAL productivity as well.^{27, 29, 35} It has been reported that the interactions of laser pulses and fabricated NPs are minimized for liquid layers smaller than 1.2 mm as a consequence of the short optical path involved.^{27, 29} Moreover, this interaction can also be influenced by the wavelength of the laser used. For laser wavelengths in the infrared region this interaction is minimized for most of the materials and a saturation in NP productivity as a consequence of scattering and post irradiation of the generated NPs cannot be observed.³¹ It follows that most of the laser energy is used for the ablation process. In comparison with the fundamental wavelength a saturation in the ablation efficiency can be observed for silver using a second harmonic generated wavelength of the laser due to its higher absorption, which is close to the surface plasmon resonance (SPR) causing fragmentation of the particles.³¹

In principle, if all these cost-intensive and non-cost-intensive parameters are optimized and combined NP productivity higher than 1 g/h could be feasible. Sajti et al.¹⁷ achieved ablation rates of 1.3 g/h for an ablation time of 30 min with α -Al₂O₃ pressed bulk-targets. During real one

hour ablation synthesis in liquid flow with a high-power and high repetition rate laser NPs productivities up to 4 g/h for gold and platinum could be reached.^{25, 26} But if a bulk target (foil or sheet) is used, one has to deal with some drawbacks. For instance, with a limited ablation time which always exist because of the laser induced generation of craters onto the target surface. Moreover, causing interruption of the production process because of target replacement, the generated craters on the target also influence the focus position and thus the NP productivity during the ablation process.^{28, 31, 36} These drawbacks prevent a completely continuous ablation process. For this reason, a promising approach to scale-up and realize a continuous ablation process can be represented by the use of a continuously fed wire target.²⁰ Messina et al.²⁰ showed that for silver wires with different diameters the observed NP productivity is higher than during the ablation of a bulk target. Furthermore, the dynamics and shape of the cavitation bubble (spherical, enwrapping the wire) differs with the cavitation bubble (hemispherical) at a bulk target.^{19, 33} This is an explanation for the observed higher NP productivity. Due to the small size of the wires the change in the focus position during the ablation process is limited. Altogether, this allows a uniform continuous ablation of the material retaining both NP quality and productivity.

In this work, we present a new setup in which continuously fed wires used for the ablation process are combined with a small liquid layer thickness. Small liquid layers were realized with a jet construction, which was inspired by the literature on laser fragmentation of dispersed particles.^{37, 38} Here, wires with different diameter covered by a free liquid jet layer are ablated by a nanosecond laser. The influence of the liquid layer thickness on the NP productivity is studied. It should be considered that the simplicity of this setup, which does not need an ablation chamber with windows and sealings, adds more perspectives for its scaling-up towards large scale

production of NPs. From the outcomes of this work a further step towards the development of a fully continuous PLAL process for upscaling purposes is determined.

Experimental Section

The experimental setup used in this work for the wire ablation is shown in Fig. 1. Different wires (materials and diameters) were continuously fed by a wire feeder inserted-in the jet-module. In this module the wire was in contact with the liquid and it was wrapped by a liquid layer which could be varied by using different nozzles from 1 to 4 mm in diameter.

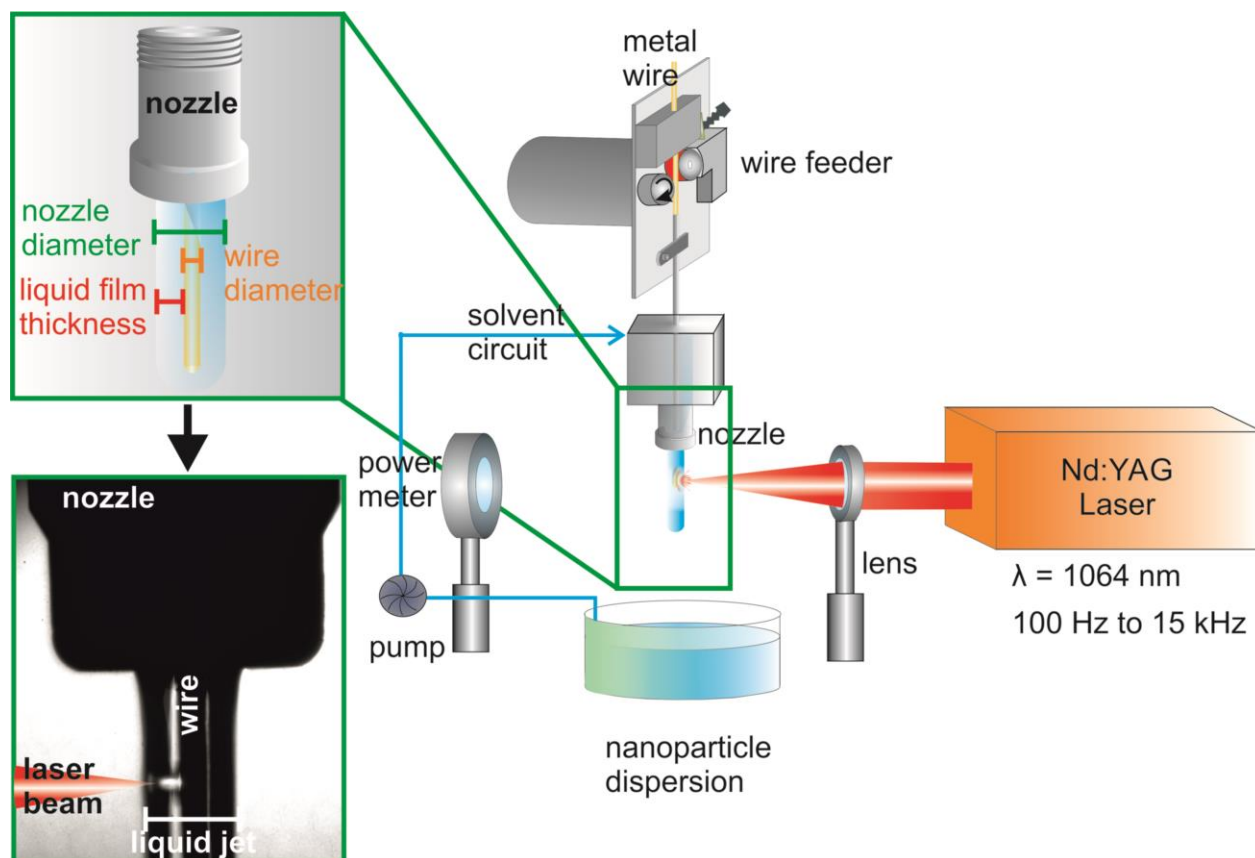


Figure 1: Schematic sketch of the experimental setup for continuous wire ablation in a small liquid jet.

The liquid layer thickness was evaluated using a mobile camera system (Euromex Camera VC.6500) for imaging acquisitions and the software ImageJ for their analysis. The water flow

was controlled by a pump concurrent to the wire feeding direction with a flow rate of up to 8 mL/s. In order to acquire shadowgraphic images a Princeton Instruments ICCD PI MAXII equipped with a UV-Vis Nikkor lens and the setup of Refs.^{20,33} were used.

The laser beam of the used nanosecond Nd:YAG laser (Rofin RSM 100D) was focused on the wire wrapped by the liquid jet by a lens ($f = 100$ mm). Pulse energies and repetition rates used in this work ranged from 2 to 8 mJ and 100 Hz to 15 kHz, respectively. To ensure the optimal alignment (center) of the laser beam onto the wire surface, the energy of the laser passing beyond the wire was measured by a power meter (Ophir Photonics nova) placed behind the wire position. In this manner the laser energy passing the wire has been minimized so that the most efficient experimental conditions could be determined. To ensure a complete irradiation of the different wires the focal lens position was finely tuned reaching, for all wires, the minimum of the measured laser energy.

Nanoparticle productivity investigations have been carried out using silver wires of different diameters (250 μm , 350 μm , 500 μm and 750 μm) and different liquid layer thicknesses. To investigate the influence of the target material on the productivity, platinum, gold, copper and aluminium wires of the same diameter (500 μm) have been used. A pulse energy of 6.5 mJ was employed for these experiments in order to reach the ablation threshold of 1.5 J/cm² required for all wires.²⁰ Moreover, these results have been compared with those obtained for the ablation of bulk targets of the same materials, performed in a flow chamber.

The ablation rate or NP productivity could be affected by changing the wire feeding speed, which has been varied by the software-controlled turning speed of the wire feeder. Therefore, the process was operated in a steady state condition. This means that the wire feeding speed was chosen in such a manner that a complete ablation of the wire (100% efficiency) in the liquid

filament was possible. From the feeding speed, the diameter and density of the wire, it was possible to calculate the ablated mass and mass per unit of time (mg/h). The verification of this procedure was demonstrated following the gravimetric determination used by Messina et al.²⁰. For comparison of the calculated ablation rates with the NP yield the generated colloidal solutions were analysed via UV-Vis extinction spectroscopy (ThermoScientific Evolution 201) using a quartz cuvette with 10 mm optical path length, calibrated with NP concentration.

Results and Discussion

Optimization of laser parameters

The ablation efficiency and NP productivity is influenced by the laser parameters as well as by the material. To get the highest possible NP productivity it is crucial to optimize laser parameters such as the repetition rate and the pulse energy. Fig. 2b demonstrates the influence of the pulse energy applied to the wire on the NP productivity, using a 350 μm silver wire and a focal position enabling 100 % ablation of the wire. The NP productivity increases with higher laser pulse energies and can be described with a rising exponential function.

By changing the repetition rate of the laser system and keeping the pulse energy at a value of 5.5 mJ (fluence = 11.2 J/cm²) the influence of the repetition rate on the NP productivity has been followed (Fig. 2a). The laser repetition rate was varied from 100 Hz to 15 kHz. Fig. 2 a shows the ablation efficiency per pulse and the NP productivity as function of the repetition rate. The silver wire (250 μm) was irradiated for 4 min for every measurement and the NP productivity was calculated by the feeding speed of the wire. The diagram can be distinguished in two regions.

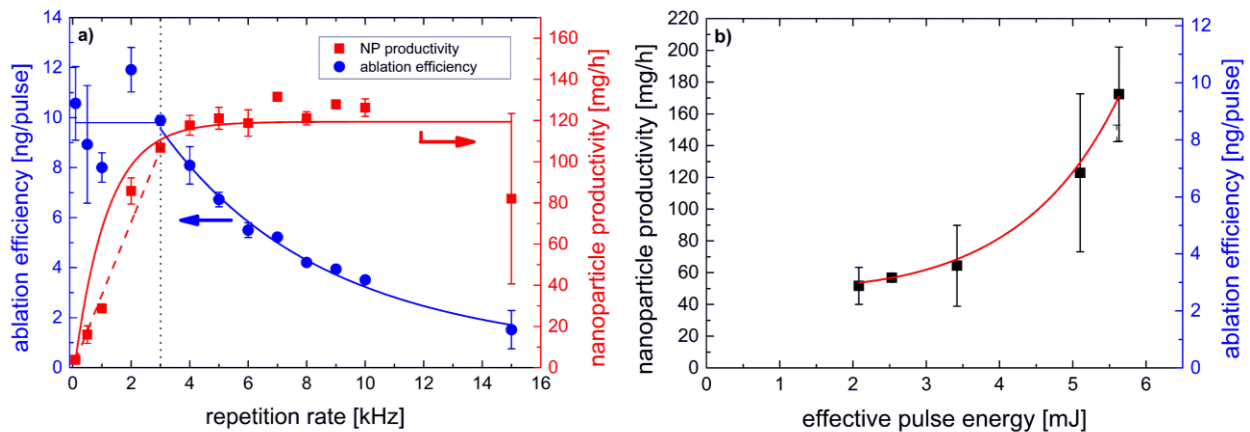


Figure 2: Ablation efficiency and NP productivity as a function of the repetition rate of the laser system (a) (pulse energy 5.5 mJ, wire diameter 250 μm , liquid flow: 3 mL/s) and as a function of the applied pulse energy of the laser (b) (repetition rate 5 kHz, wire diameter 350 μm , liquid flow: 3 mL/s). Below 3 kHz the ablation efficiency is constant and consequently the NP productivity as a function of the repetition rate is nearly linear in this region. For repetition rates higher than 3 kHz the ablation efficiency decreases exponentially connected with a flattening of the NP productivity to a final saturation.

For low repetition rates (< 3 kHz) the ablation efficiency forms a plateau and all data belong to the same region. By increasing the repetition rate (> 3 kHz) the ablation efficiency decreases exponentially. In the first regime, the productivity increases linearly (dotted line) with repetition rate up to a smooth transition when a saturation is observed. For a bulk target a similar behaviour was reported by Wagener et al.²⁸ They investigated the ablated mass by controlling the spatial and temporal interpulse distance. Wagener et al.²⁸ attributed the saturation of productivity and the decrease in the ablation efficiency with the shielding effect of the generated cavitation bubble, due to the fact that the lifetime of the cavitation bubble is in the time-regime of the temporal interpulse distance. This shielding results in a decrease in the NP productivity because of the absorption and scattering of the laser beam by the cavitation bubble itself.^{17, 28} Therefore, the lifetime of the cavitation bubble on the wire is approximately determined by a repetition rate-related investigation of the ablation efficiency as it is shown in Fig. 2. Assuming that only the cavitation bubble shields the laser pulse, the cavitation bubble life-time is determined by the

starting point of the exponential decrease of the ablation efficiency. For repetition rates smaller than 3 kHz a constant ablation efficiency is obtained. In this region the cavitation bubble has already collapsed when the subsequent laser pulse is hitting the wire.

For the determination of the life-time of the cavitation bubble it is useful to convert the experimental data from frequency into a unit of time (see Fig. S1). The exponential productivity decrease is observed in a repetition rate interval of around 3 kHz which corresponds to an interpulse delay and thus a cavitation bubble life-time of about 330 μs (assuming that mainly the cavitation bubble shields the laser pulse). This calculated lifetime of the cavitation bubble is significantly longer than the lifetimes found for ns-laser pulses in the literature.^{32, 33} Sasaki et al.³² observed a bubble life-time of 190 μs , at ambient pressure (using 22 mJ of a ns pulse). This means, in comparison with our experiments (5.5 mJ) an approximately 4-times higher laser pulse energy were used but life-time was far less. For a wire ablation the cavitation bubble dynamics and lifetime was studied via shadowgraphy by De Giacomo et al.³³. The total lifetime of the laser induced cavitation bubble was about 180 μs for a 250 μm silver wire and a comparable laser fluence of 1.4 J/cm².³³ This large difference in the calculated “ablation effective” lifetime of the bubble and the literature based on shadowgraphy strongly suggests that our initial assumption, that only the cavitation bubble itself is responsible for the shielding of the laser, is not accurate. To determine a more accurate lifetime and to investigate the dynamics of the cavitation bubble in the small liquid filament, shadowgraphic images were recorded with the same setup already described in detail in literature³³. The time resolved shadowgraphic images of the laser-induced bubble on a 750 μm silver wire in a small liquid filament (about 1.5 mm) are shown in Fig. 3. During the first 100 μs a bubble expansion with subsequent shrinking is observed. This shows its similarity to the dynamics of the cavitation bubble determined for a bulk-ablation.³³ For instance, the 750 μm silver wire displays a dynamic of the cavitation bubble in the liquid filament, which

is completely in agreement with that shown in a bigger filament by De Giacomo et al.³³. Fig. 4 shows the first bubble collapse occurring at 110 μs with a successive expansion characterized by a mushroom-shape.

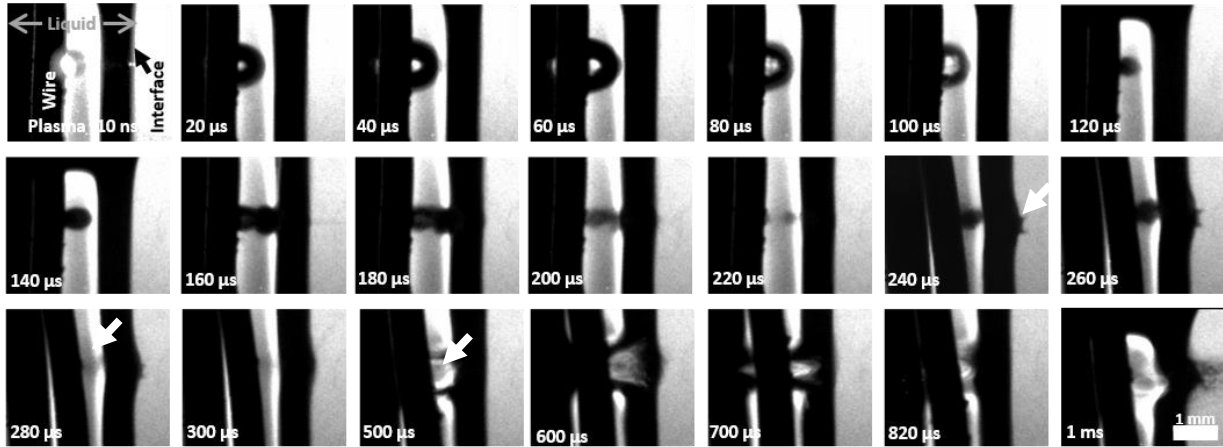


Figure 3: Time-resolved shadowgraphic images of the laser induced cavitation bubble generated on a 750 μm Ag wire in presence of a small liquid filament (3 mm nozzle diameter, flow rate: 6 mL/s, pulse energy= 6.5 mJ, gate width = 10 μs). The shadow-like cloud for 280 μs indicated by the white arrow thought to be induced small vapor bubbles. The other white arrow at a delay time of 500 μs indicating a shock-wave induced vapor bubble.

The slow displacement of the cavitation bubble away from the wire surface (in about 160 μs) also shown in the temporal evolution of the aspect ratio reported in Fig. 4. The maximum size of the bubble along the x-direction (towards the laser beam) is higher than the expansion along the y-axis (wire axis). This is a result of mechanical properties of the wire, which acts like a bow or spring board.^{19, 33} In this manner it provides a more effective ejection of the bubble and transport of the ablated material in the liquid medium. After the final collapse the generated shock-wave is back-reflected from the liquid/air interface and supplying, in first approximation, the self-generation of a vapor-bubble as can be assumed at 500 μs of Fig. 3 (marked by an arrow). In this case, however, the change of the distance between the wire and the liquid edge could involve more complex processes which will be here neglected because out of the aim of this work. After each cavitation bubble collapse a shock-wave expansion follows, so that the liquid-jet surface

(liquid air boundary) is deformed and a curvature of it is generated (e.g., at 240 μs). Nevertheless, as it is shown in Fig. 2 all these side events have no influence on the NP productivity and the relative ablation efficiency, as they appear earlier than 330 μs .

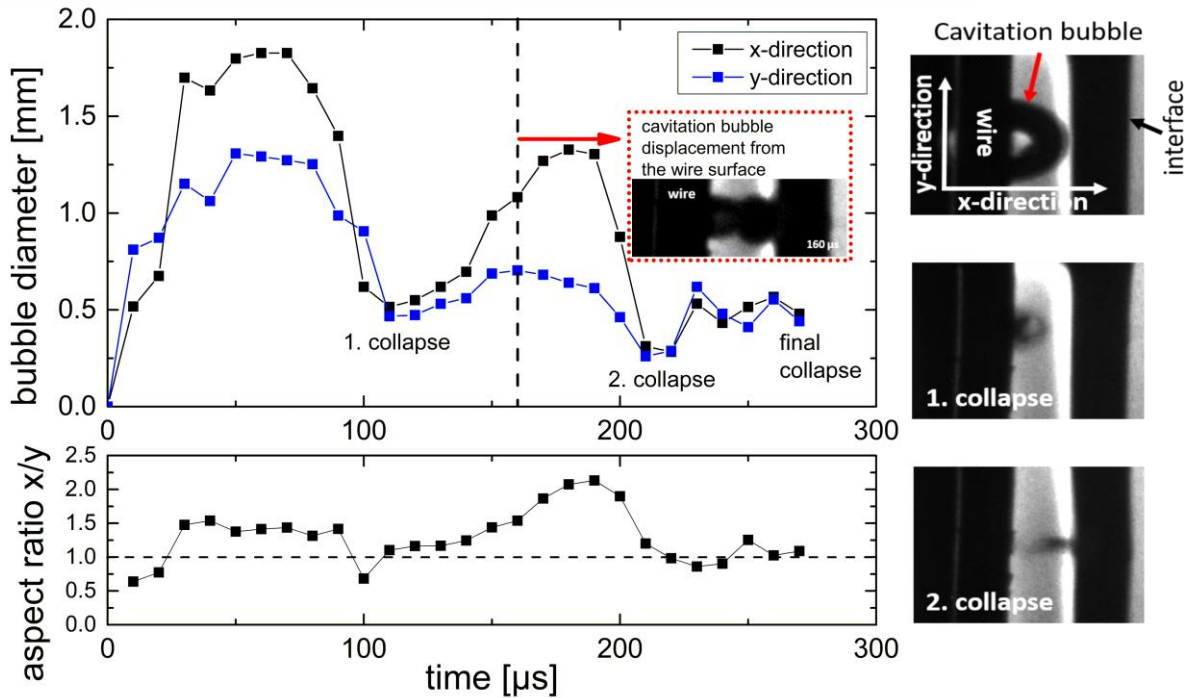


Figure 4: Temporal evolution of the laser induced cavitation bubble generated on a 750 μm Ag wire in presence of a small liquid filament (measured from Fig. 3). The diagram shows the oscillation of the cavitation bubble inside the small liquid filament and the trend of the aspect ratio. Additional shadowgraphic images of the 1. and 2. collapse of the bubble are presented on the right.

By means of Fig. 4 we could determine the cavitation bubble oscillation life-time of 270 μs until final collapse. The difference between the calculated cavitation bubble life-time (around 330 μs , which correlates to the end of the described plateau of Fig. 2 a) and the one detected via shadowgraphic images that is 270 μs , suggests that the shielding of the laser pulse is led by the complexity of the process itself. It can be hypothesized that the ablated material and successive oscillating and decreasing in size cavitation bubbles have an influence on this shielding together with the other components induced by the process that are NPs and self-generated small vapor

bubbles.³⁴ This effect is schematically shown in Fig. 5. During the life-time (270 μ s) of the cavitation bubble a shielding of the laser may occur primarily by the same bubble. After its collapse the shielding could occur through the generated NPs as well as the small vapor bubbles which are released or formed in the liquid at different time ranges.

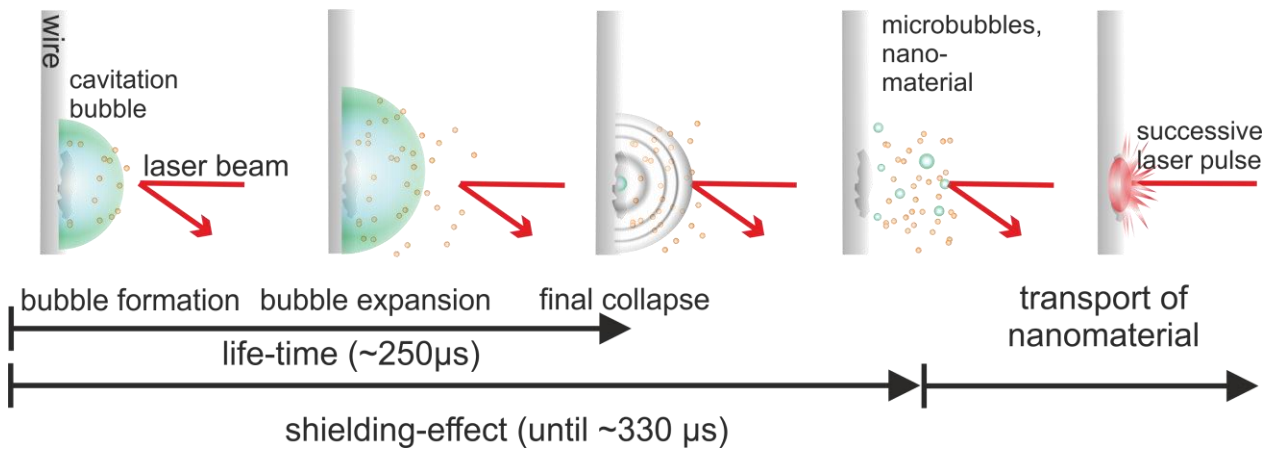


Figure 5: Schematic illustration of the shielding effect.

The NPs are trapped in the mushroom-shaped bubble (Fig. 3 160 μ s) and are released into the liquid after 270 μ s (final collapse). The interaction of suspended particles and the laser pulse during multiple-shot irradiation was also demonstrated by Tanabe et al.³⁹. They found that the formation of small (micrometer-sized) bubbles induced by the interaction of the laser pulse with generated NPs results in a decreasing laser pulse energy reaching the target. In Fig. 3 at 280 μ s a cloud like shadow can be presumed, thought to represent these small vapor bubbles. The loss of the laser energy by scattering or absorption of the generated NPs is material- and laser-wavelength dependent. Schwenke et al.³¹ observed that the cumulative ablated mass increases linearly for a silver target using the fundamental laser wavelength. However, for zinc an interaction with the 1064 nm laser is observed which induces a decrease in the NP productivity and a saturation in the cumulative ablated mass follows.³¹ This effect is reduced if a more effective transportation of the ablated material and self-generated small vapor bubbles is involved

such as the presence of a liquid flow. Consequently, as it is schematically shown in Fig. 5, a successive laser pulse can act more effectively if the generated NPs and self-generated small vapor bubbles are transported away from the ablation spot in the liquid. A further way to minimize this effect might be by means of reduction of the optical path by employing thinner liquid layers.

Influence of the liquid layer thickness and wire diameter

Besides the optimization of the NP productivity by varying the laser parameter, a (non-cost-intensive) productivity increase can also be realized by changing system or setup-parameters. For instance, for our setup, we were able to vary the liquid layer thickness surrounding the wire surface. In order to evaluate the role of the liquid layer thickness in increasing the NP productivity, its thickness was varied by employing different diameters of the applied nozzles. In Fig. 6 the influence of the water layer thickness on NP productivity for different silver wires is summarized for a laser pulse energy of 6.5 mJ with a 5 kHz laser repetition rate, a continuous liquid flow of 8 mL/s and a liquid volume of 400 mL. A repetition rate of 5 kHz was employed in order to ensure the highest stability and pulse energies of the laser system in use. This was due to the necessity of reaching the ablation threshold of 1.5 J/cm² needed for all silver wires employed here.²⁰ Additionally, to reduce the influence of the generated NPs and their properties (SPR, absorption@1064 nm, agglomeration), on the NP productivity as well as to facilitate the particle analysis, 1 mM sodium citrate was added to the solutions. TEM images and size distribution diagram of citrate stabilized silver NPs, generated in the liquid jet, are shown in Fig. S8. The size distribution is bimodal with two average NP diameters of 2 and 8 nm (from lognormal Fit).

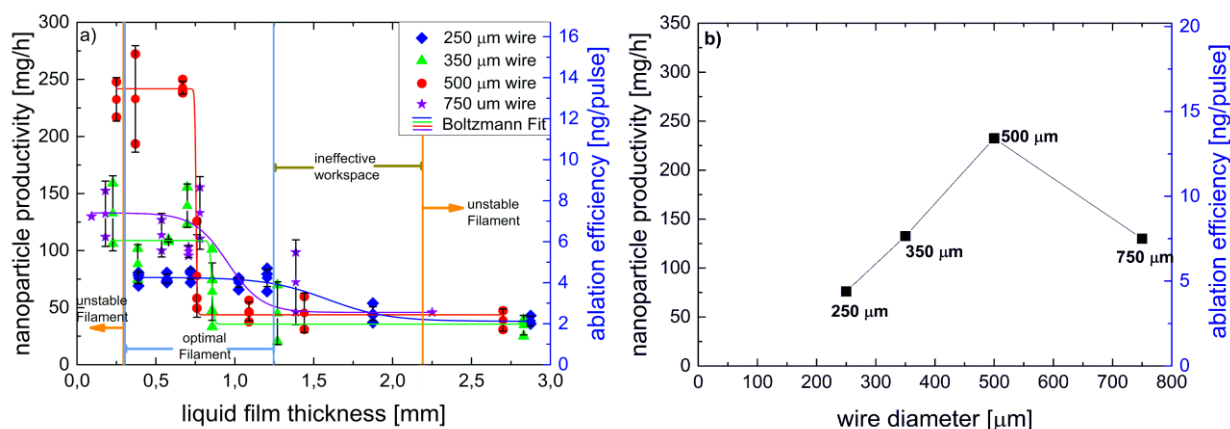


Figure 6: a) Evolution of the NP productivity and ablation efficiency for the variation of the liquid layer thickness and silver wire diameters (250 μm , 350 μm , 500 μm , 750 μm). b) NP productivity and ablation efficiency as function of the wire diameter for a 0.6 mm liquid layer. Repetition rate: 5 kHz, pulse energy: 6.5 mJ, liquid flow: 8 mL/s.

The liquid layer was changed by the diameter of the nozzle. A 5-times increase in ablation rate from 46 mg/h to 243 mg/h was observed during the ablation of the 500 μm thickness silver wire through reducing the liquid layer, or otherwise related nozzle diameter, from 1000 μm to 700 μm , respectively. This enhancement of the ablation rate was observed for all applied wire diameters. Nevertheless, a limitation in the reduction of the liquid layer thickness was observed. As it is reported in Fig. S2, for a layer smaller than 0.3 mm an irregular ablation was determined from the UV-Vis-spectra and the peak intensity at 400 nm did not correlate with the ones related to the expected NP productivity. Less silver was analysed in the colloid than ablated from the wire. In fact, the deviations observed in this region (deviation of 15.5 %) are much higher than those due to thicker liquid layers (deviation from 6.5 to 8.7 %). Consequently, for this, a partially ablation in air might have occurred and the NPs were not captured in the solvent, which was used for the UV/Vis measurements. This effect was also observed in the case shown in Fig. S3, where the flow rate was decreased. For flow rates lower than 3 mL/s the measured absorbance differs from the absorbance calculated by the ablated mass. In extreme, if the liquid layer thickness is below 0.3 mm and a low flow rate (< 3 mL/s) is set, the liquid layer is destroyed by the impinging laser.

This is also noticed by the occurrence of a more intense plasma which indicates a partial ablation in air.

A positive effect of the liquid layer thickness was reported by Bärsch et al.²⁷, who investigated the influence of different thicknesses of acetone layer on ablation rate during the ablation of a zirconia target. The highest ablation efficiencies of zirconia could be observed for a liquid layer smaller than 0.8 mm, which is in a good agreement with our experiments. Moreover, Jiang et al.²⁹ found the highest productivity for an “optimal” water layer thickness of 1.2 mm using a germanium target and a 532 nm laser system. The NP productivity can be influenced by the pressure due to the expanding laser induced plasma. This pressure can be increased by enlarging the confining liquid layer thickness. In comparison with ablation in air the plasma-pressure can be several orders of magnitude higher with a confining liquid⁴⁰ and the duration of the shock wave can last 2-3- times longer leading to higher NP productivity³⁵. The liquid layer confines the plasma and its expansion can be delayed.⁴¹ Despite the induced higher plasma pressure due to thicker liquid layers a decrease of the NP productivity is observed. On one hand, it should be considered that for very thin liquid layers the optical path becomes shorter. Moreover, in case of our experiments the liquid was circulating continuously. Thus, an interaction between the generated NPs and the laser pulse could take place. This causes a reduction of the pulse energy that reaches the wire surface as Mafuné et al.⁴² found for the generation of gold NPs using a 1064 nm laser. In such circumstances saturation could occur after several thousands of laser shots due to the laser absorption by the generated gold NPs.

On the other hand, the cavitation bubbles and shock wave induced after the ablation process oscillates between the liquid-air interface⁴³ (e.g. Fig. 3 and Fig. S4) and the wire surface, where part of their energy is dissipated. In the same manner also shockwaves induced by laser induced

plasma (during the first ns after the laser pulse) can give a contribution since, as it is reported by Vogel et al.⁴⁴, part of the energy of the laser is transformed in the energy of shockwaves. The propagation of these components between the liquid and the target surface, in the time of some hundreds of microseconds, may promote (plasma heating) the release of further material.^{18, 28, 45} It has been evidenced that for all liquid layers a back-reflection of the cavitation bubbles at the interface is observed. The energy loss of it propagating in the liquid jet depends on the liquid jet features, its distance from the wire surface and phase interface. With thicker liquid layers the shockwave loose most of their energy towards the liquid.

Moreover, if a very thin liquid layer is used, the cavitation bubbles front reach quickly the liquid-air interface where it remains trapped so that the back-reflected part can provide a more complex process where some mechanical effects onto the wire surface are induced and additional detachments of the material can occur from this, which is reported in detail in the literature⁴⁶. Overall, the optimum in NP productivity is observed for liquid layer around 0.6 mm for all wire diameters which also provides a stable operation and ablation of the wire materials.

In addition to the liquid layer, the wire diameter was varied during the experiments as reported in Fig. 5. The highest NP productivity was determined for a wire diameter of 500 μm . For this diameter the stability of the process was increased in comparison with smaller wire diameters. Messina et al. found the highest NP productivity for a silver wire diameter of 750 μm . For wire diameters lower than 750 μm they observed a significantly reduced ablation efficiency and several effects which should be responsible for this decrease were discussed. On one hand a higher surface to volume ratio occurring for thinner wires can support a more effective heat dissipation through the surrounding liquid.²⁰ For thicker ones ($>750 \mu\text{m}$) this effect can be decreased because wires act in a very similar way than a bulk target.

Moreover, since the laser reflectivity of a metal wire depends on its diameter it follows that a less effective absorption of the laser energy occurs for thinner ones.²⁰ Although, for wires thicker than 900 μm the dynamics of the induced cavitation bubbles is comparable with those of a bulk-target.³³ This is affected by the laser power used as well as the maximum bubble size³³. For experiments here reported fluences in the range of 1.5 - 14 J/cm^2 were used that are lower than those used by De Giacomo et al. (68 J/cm^2). It has been observed that the change in the cavitation bubble dynamics can be observed for wire diameters lower than 900 μm . For instance, Fig. 3 shows that for the 750 μm wire the cavitation bubble shapes are similar to the ones occurring at a bulk target. The change in the cavitation bubbles dynamics can be a reason for lower NP productivity in case of a 750 μm wire ablation at the moderate fluences used here, and the optimum at 500 μm silver wire diameter.

Furthermore, the effect described by Kohsakowski et al.¹⁹ and De Giacomo et al.³³ where the wire behaves like a spring board or a bow, can affect the NP productivity depending on both the wire diameter and elasticity of the material. The effective transportation of the ablated material is shown in the shadowgraphic images of Fig. 3. For instance, after 160 μs the cavitation bubble starts to displace from the wire surface changing into a mushroom like shape. This change in shape is due to the spring-board like behaviour of the wire.¹⁹ It follows that after the first cavitation bubble collapse the wire is deflected from its initial position. Due to its elasticity the wire tends to return to the initial position causing the displacement of the cavitation bubble from its surface. For a thicker wire diameter, the transportation of the material in the liquid caused by this effect, when its elasticity approaches to a bulk-target is not effective anymore.

Chamber design and target geometry for scale-up

Small liquid layers provide an enhancement of the ablation process and consequently an increase in NP productivity thanks to the limited interaction taking place between the laser pulse and the previously generated microbubbles and NPs which is in turn reduced because of the limited optical pathway of liquid involved.

In comparison with the ablation in a conventional batch chamber a continuous ablation in an equivalent volume is observed over 1 hour for ablation in a wire-jet geometry where the same laser parameters and a volume of 100 ml of deionized water with 1mM sodium citrate were used (Fig. 7). In case of the ablation process in the liquid jet, the obtained colloidal solution was continuously re-circulated. During the bulk target ablation, the mass was determined both gravimetrically and via UV-Vis measurements. For the wire ablation in the liquid jet the ablated mass was evaluated by the UV-Vis data whose concentration was in a good correlation with the absorbance at 320 nm which increased linearly with the ablation time and NP productivity.

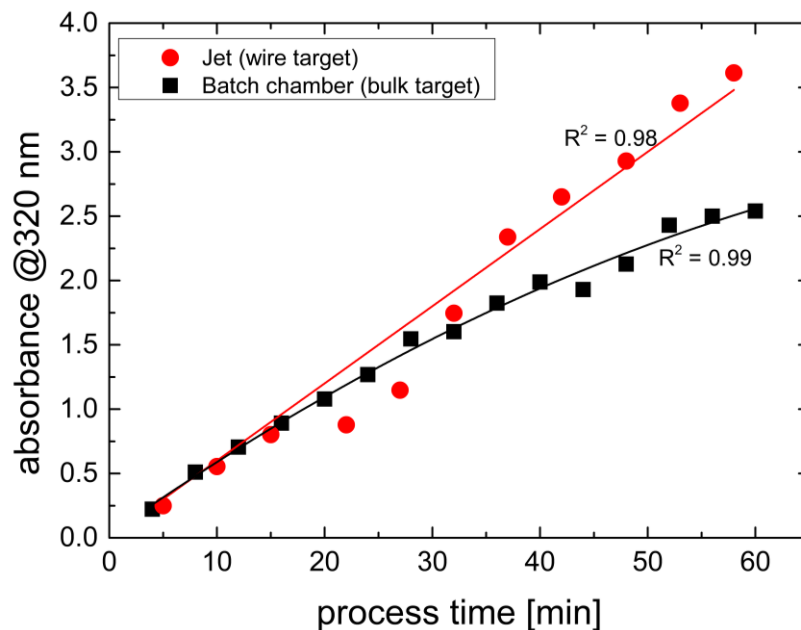


Figure 7: Comparison of the NP productivity for the wire ablation in the liquid jet and for a common bulk target ablation performed in a batch chamber. Data determined by the absorbance of the silver colloids at 320 nm.

Comparing the ablation in the small liquid filament of 0.6 mm with the one performed in the batch chamber with 5 mm liquid layer, it has been evidenced that already after 20 minutes the NP's absorbance reached their saturation value in the batch. It should be mentioned that Schwenke et al.³¹ have not observed a significant effect on the ablation efficiency of the generated silver NPs if a 1064 nm picosecond laser was used during 60 minutes. Nevertheless, increasing the concentrations of silver NPs the number of agglomerates and aggregates increased. The formation of agglomerates and aggregates has also been evidenced by taking into account the UV-Vis absorbance data around 800 nm reported in Fig S5. In this region the absorbance is in a good agreement with the concentration of either agglomerates or aggregates of NPs.⁴⁷ These interact with the incident laser beam reducing its energy reaching to the silver target. For both, the ablation in the batch chamber and in the liquid jet, the absorbance at 800 nm increased by a factor of 6-7 during the 1 hour ablation. This increase in the concentration of agglomerates and aggregates can be considered to be responsible for the saturation of the NP productivity occurring

during the ablation performed in the batch chamber. In contrary, up-concentration at the colloid during wire ablation in liquid jet was not limited within 60 min, reaching a concentration of 900 mg/mL.

In addition to the higher NP productivity and higher final concentration compared to the batch, it should be highlighted that the wire ablation in the liquid jet can be carried in a continuous process since the wire is regularly fed into the laser focus. On the contrary, for the batch chamber the metal target position has to be changed if some craters or other surface's irregularities affecting the NP productivity are present. This means that, if it is needed the process or the focus position has to be stopped or corrected. In order to realize NP productivities comparable with other well established methods the ablation of the wire and its scaling-up can be adopted. In fact, thanks to its form, the requirement that continuous feeding of material needed for reaching a high efficiency of the process can be fulfilled. Moreover, it has been noted that NP productivities obtained for all different applied materials and wire diameters are higher, as it is reported in Fig. S6, than those observed in a liquid flow chamber ablating a bulk target.

Conclusion

This work demonstrates that the laser ablation of wires in a thin liquid jet is a promising approach to realize a continuous ablation process with efficient ablation rates and NP productivities. In our setup we combined two non-cost-intensive approaches to increase the NP productivity – a thin liquid layer and a wire shaped target. In fact, in these circumstances higher NP productivities in comparison with the ablation of a bulk target in a batch or flow chamber are observed. Highest NP productivities were determined for liquid layers smaller than 600 μm (1700 μm liquid nozzle) whereas the ablation of a 500 μm silver wire was most effective. The dynamics of the cavitation bubbles observed in the thin liquid jet shows that these remain inside the liquid layer causing its

curvature after collapsing and propagation towards the air-liquid phase boundary. Moreover, the ablated material is dispersed more efficiently into the liquid when the mechanical flexibility of the wire can play a role in transferring kinetic energy to propagating bubble transporting the NPs. In addition to the thin liquid layer and the wire-shaped target the NPs are removed more efficiently downwards from the wire surface thanks to the liquid flow which is another advantage of the presented setup. In comparison with the popular ablation of the target in a batch chamber this setup shows the advantage of short optical path of the laser through the liquid minimizing its effect and providing a continuous linear productivity of NPs. In contrast to this, a saturation in the NP productivity is observed in case of performing the ablation in the batch chamber but not in liquid jet re-circulation setup, reaching higher concentrations. It has been also demonstrated that the laser pulse is not only shielded by the formed cavitation bubbles and their rebounds but even from the produced NPs as well as small self-generated vapor bubbles (dispersed microbubbles). These additional shielding effects result in both a saturation in the NP productivity and in a decrease of the ablation efficiency at repetition rates higher than 3 kHz.

It follows that the wire ablation in a small liquid filament is a promising approach to realize and develop a continuous ablation process providing another step for scaling-up the process towards industrial application where a high mass production of ligand-free silver NPs could be required in a robust manner. Furthermore, by the simple substitution of the wire material used the generation of NPs of other kind can also be achieved.

Acknowledgement

This study was supported by the German federal ministry of education and research (BMBF) within the young investigator competition NanoMatFutur (project INNOKAT, FKZ 03X5523)

Associated Content

Supporting Information. Further information on the characterization of the laser-generated Ag-NPs, ablation efficiencies diagrams as function of the flow-rate and interpulse distance and additional comparative diagrams can be found within the Supporting Information.

References

- [1] Kammler, H. K.; Mädler, L.; Pratsinis, S. E. Flame Synthesis of Nanoparticles. *Chem. Eng. Technol.* **2001**, *24*, 583–596.
- [2] Swihart, M. T. Vapor-phase synthesis of nanoparticles. *Curr. Opin. Colloid Interface Sci.* **2003**, *8*, 127–133.
- [3] Brust, M.; Walker, M.; Bethell, D.; Schiffrin, D. J.; Whyman, R. Synthesis of thiol-derivatised gold nanoparticles in a two-phase Liquid-Liquid system. *J. Chem. Soc., Chem. Commun.* **1994**, 801–802.
- [4] Turkevich, J.; Stevenson, P. C.; Hillier, J. A study of the nucleation and growth processes in the synthesis of colloidal gold. *Discuss. Faraday Soc.* **1951**, *11*, 55–75.
- [5] Mende, S.; Stenger, F.; Peukert, W.; Schwedes, J. Production of sub-micron particles by wet comminution in stirred media mills. *J. Mater. Sci.* **2004**, *39*, 5223–5226.
- [6] Barcikowski, S.; Compagnini, G. Advanced Nanoparticle Generation and Excitation by Lasers in Liquids. *Phys. Chem. Chem. Phys.* **2013**, *15*, 3022–3026.
- [7] Lin, F.; Yang, J.; Lu, S.-H.; Niu, K.-Y.; Liu, Y.; Sun, J.; Du, X.-W. J. Laser synthesis of gold/oxide nanocomposites. *Mater. Chem.* **2010**, *20*, 1103–1106.
- [8] Tong, H.; Ouyang, S.; Bi, Y.; Umezawa, N.; Oshikiri, M.; Ye, J. Nano-photocatalytic Materials: Possibilities and Challenges. *Adv. Mat.* **2012**, *24*, 229–251.
- [9] Samuel, U.; Guggenbichler, J. Prevention of catheter-related infections: the potential of a new nano-silver impregnated catheter. *Int. J. Antimicrob. Ag.* **2004**, *23*, Supplement 1, 75–78.
- [10] Beck, A.; Horvath, A.; Schay, Z.; Stefler, G.; Koppany, Z.; Sajo, I.; Geszti, O.; Guzzi, L. Sol derived gold-palladium bimetallic nanoparticles on TiO₂: structure and catalytic activity in CO oxidation. *Top. Catal.* **2007**, *44*, 115–121.
- [11] Balasubramanian, S. K.; Poh, K.-W.; Ong, C.-N.; Kreyling, W. G.; Ong, W.-Y.; Yu, L. E. The effect of primary particle size on biodistribution of inhaled gold nano-agglomerates. *Biomater.* **2013**, *34*, 5439–5452.
- [12] Amendola, V.; Meneghetti, M. Laser ablation synthesis in solution and size manipulation of noble metal nanoparticles. *Phys. Chem. Chem. Phys.* **2009**, *11*, 3805–3821.
- [13] Hahn, A.; Barcikowski, S. Production of Bioactive Nanomaterial Using Laser Generated Nanoparticles. *JLMN - Journal of Laser Micro / Nanoengineering* **2009**, *4*, 51–54.

- [14] Jakobi, J.; Menendez-Manjon, A.; Chakravadhanula, V. S. K.; Kienle, L.; Wagener, P.; Barcikowski, S. Stoichiometry of alloy nanoparticles from laser ablation of PtIr in acetone and their electrophoretic deposition on PtIr electrodes. *Nanotechnology* **2011**, *22*, 145601 (7pp).
- [15] Neumeister, A.; Jakobi, J.; Rehbock, C.; Moysig, J.; Barcikowski, S. Monophasic ligand-free alloy nanoparticle synthesis determinants during pulsed laser ablation of bulk alloy and consolidated microparticles in water. *Phys. Chem. Chem. Phys.* **2014**, *16*, 23671–23678.
- [16] Oko, D. N.; Zhang, J.; Garbarino, S.; Chaker, M.; Ma, D.; Tavares, A. C.; Guay, D. Formic acid electro-oxidation at PtAu alloyed nanoparticles synthesized by pulsed laser ablation in liquids. *Journal of Power Sources* **2014**, *248*, 273 – 282.
- [17] Sajti, C. L.; Sattari, R.; Chichkov, B. N.; Barcikowski, S. Gram Scale Synthesis of Pure Ceramic Nanoparticles by Laser Ablation in Liquid. *J. Phys. Chem. C* **2010**, *114*, 2421–2427.
- [18] Amendola, V.; Meneghetti, M. What controls the composition and the structure of nanomaterials generated by laser ablation in liquid solution? *Phys. Chem. Chem. Phys.* **2013**, *15*, 3027–3046.
- [19] Kohsakowski, S.; Gökce, B.; Tanabe, R.; Wagener, P.; Plech, A.; Ito, Y.; Barcikowski, S. Target geometry and rigidity determines laser-induced cavitation bubble transport and nanoparticle productivity - a high-speed videography study. *Phys. Chem. Chem. Phys.* **2016**, *18*, 16585–16593.
- [20] Messina, G. C.; Wagener, P.; Streubel, R.; De Giacomo, A.; Santagata, A.; Compagnini, G.; Barcikowski, S. Pulsed laser ablation of a continuously-fed wire in liquid flow for high-yield production of silver nanoparticles. *Phys. Chem. Chem. Phys.* **2013**, *15*, 3093–3098.
- [21] Chewchinda, P.; Odawara, O.; Wada, H. The effect of energy density on yield of silicon nanoparticles prepared by pulsed laser ablation in liquid. *Appl. Phys. A* **2014**, *117*, 131–135.
- [22] Kalyva, M.; Bertoni, G.; Milionis, A.; Cingolani, R.; Athanassiou, A. Tuning of the characteristics of Au nanoparticles produced by solid target laser ablation into water by changing the irradiation parameters. *Microsc. Res. Tech.* **2010**, *73*, 937–943.
- [23] Kim, K. K.; Kim, D.; Kim, S. K.; Park, S. M.; Song, J. K. Formation of ZnO nanoparticles by laser ablation in neat water. *Chem. Phys. Lett.* **2011**, *511*, 116 – 120.
- [24] Sajti, C. L.; Sattari, R.; Chichkov, B. N.; Barcikowski, S. Ablation efficiency of alpha-Al₂O₃ in liquid phase and ambient air by nanosecond laser irradiation. *Appl. Phys. A* **2010**, *100*, 203–206.
- [25] Streubel, R.; Barcikowski, S.; Gökce, B. Continuous multigram nanoparticle synthesis by high-power, high-repetition-rate ultrafast laser ablation in liquids. *Opt. Lett.* **2016**, *41*, 1486–1489.

- [26] Streubel, R.; Bendt, G.; Gökce, B. Pilot-scale synthesis of metal nanoparticles by high-speed pulsed laser ablation in liquids. *Nanotechnology* **2016**, *27*, 205602.
- [27] Bärsch, N.; Gatti, A.; Sattari, R.; Barcikowski, S. Improving Laser Ablation of Zirconia by Liquid Films: Multiple Influences of Liquids on Surface Machining and Nanoparticle Generation. *JLMN* **2009**, *4*, 66–70.
- [28] Wagener, P.; Schwenke, A.; Chichkov, B.; Barcikowski, S. Pulsed Laser Ablation of Zinc in Tetrahydrofuran: Bypassing the Cavitation Bubble. *J. Phys. Chem. C* **2010**, *114*, 7618–7625.
- [29] Jiang, Y.; Liu, P.; Liang, Y.; Li, H.; Yang, G. Promoting the yield of nanoparticles from laser ablation in liquid. *Appl. Phys. A* **2011**, *105*, 903–907.
- [30] Zeng, X.; Wang, Z.; Liu, Y.; Ji, M. γ -Fe₂O₃ nanoparticles prepared by laser ablation of a tiny wire. *Appl. Phys. A* **2005**, *80*, 581–584.
- [31] Schwenke, A.; Wagener, P.; Nolte, S.; Barcikowski, S. Influence of processing time on nanoparticle generation during picosecond-pulsed fundamental and second harmonic laser ablation of metals in tetrahydrofuran. *Appl. Phys. A* **2011**, *104*, 77–82.
- [32] Sasaki, K.; T., N.; Soliman, W.; Takada, N. Effect of Pressurization on the Dynamics of a Cavitation Bubble Induced by Liquid-Phase Laser Ablation. *Appl. Phys. Exp.* **2009**, *2*, 0465011–0465013.
- [33] De Giacomo, A.; Dell’Aglia, M.; Santagata, A.; Gaudiuso, R.; De Pascale, O.; Wagener, P.; Messina, G. C.; Compagnini, G.; Barcikowski, S. Cavitation dynamics of laser ablation of bulk and wire-shaped metals in water during nanoparticles production. *Phys. Chem. Chem. Phys.* **2013**, *15*, 3083–3092.
- [34] Barcikowski, S.; Menendez-Manjon, A.; Chichkov, B. N.; Brikas, M.; Raciukaitis, G. Generation of nanoparticle colloids by picosecond and femtosecond laser ablations in liquid flow. *Appl. Phys. Lett.* **2007**, *91*, 0831131 – 0831133.
- [35] Fabbro, R.; Fournier, J.; Ballard, P.; Devaux, D.; Virmont, J. Physical study of laser-produced plasma in confined geometry. *J. Appl. Phys.* **1990**, *68*, 775–784.
- [36] Menendez-Manjon, A.; Wagener, P.; Barcikowski, S. Transfer-Matrix Method for Efficient Ablation by Pulsed Laser Ablation and Nanoparticle Generation in Liquids. *J. Phys. Chem. C* **2011**, *115*, 5108–5114.
- [37] Lau, M.; Barcikowski, S. Quantification of mass-specific laser energy input converted into particle properties during picosecond pulsed laser fragmentation of zinc oxide and boron carbide in liquids. *Appl. Surf. Sci.* **2015**, *348*, 22 – 29.
- [38] Wagener, P.; Barcikowski, S. Laser Fragmentation of Organic Microparticles into Colloidal Nanoparticles in a Free Liquid Jet. *Appl. Phys. A* **2010**, *101*, 435–439.

- [39] Tanabe, R.; Nguyen, T. T.; Sugiura, T.; Ito, Y. Bubble dynamics in metal nanoparticle formation by laser ablation in liquid studied through high-speed laser stroboscopic videography. *Appl. Surf. Sci.* **2015**, *351*, 327 – 331.
- [40] Saito, K.; Takatani, K.; Sakka, T.; Ogata, Y. H. Observation of the light emitting region produced by pulsed laser irradiation to a solid-liquid interface. *Appl. Surf. Sci.* **2002**, *197-198*, 56 – 60.
- [41] Berthe, L.; Fabbro, R.; Peyre, P.; Bartnicki, E. Wavelength dependent of laser shock-wave generation in the water-confinement regime. *J. Appl. Phys.* **1999**, *85*, 7552–7555.
- [42] Mafune, F.; Kohno, J.-Y.; Takeda, Y.; Kondow, T.; Sawabe, H. Formation of Gold Nanoparticles by Laser Ablation in Aqueous Solution of Surfactant. *J. Phys. Chem. B* **2001**, *105*, 5114–5120.
- [43] Utsunomiya, Y.; Kajiwara, T.; Nishiyama, T.; Nagayama, K.; Kubota, S. Pulse laser ablation at water-air interface. *Appl. Phys. A* **2010**, *99*, 641–649.
- [44] Vogel, A.; Busch, S.; Parlitz, U. Shock wave emission and cavitation bubble generation by picosecond and nanosecond optical breakdown in water. *J. Acoust. Soc. Am.* **1996**, *100*, 148–165.
- [45] Tsuji, T.; Tsuboi, Y.; Kitamura, N.; Tsuji, M. Microsecond-resolved imaging of laser ablation at solid-liquid interface: investigation of formation process of nano-size metal colloids. *Appl. Surf. Sci.* **2004**, *229*, 365 – 371.
- [46] Dell’Aglia, M.; De Giacomo, A.; Kohsakowski, S.; Barcikowski, S.; Wagener, P.; Santagata, A. Pulsed Laser Ablation of wire-shaped target in a thin water jet: effects of plasma features and bubble dynamics on PLAL process. *Phys. Chem. Chem. Phys.* **2016**, (submitted)
- [47] Rehbock, C.; Merk, V.; Gamrad, L.; Streubel, R.; Barcikowski, S. Size control of laser-fabricated surfactant-free gold nanoparticles with highly diluted electrolytes and their subsequent bioconjugation. *Phys. Chem. Chem. Phys.* **2013**, *15*, 3057–3067.

TOC graphic:

